J|A|C|S
ARTICLES
Published on Web 12/10/2005

Orientation and Conformational Preference of Leucine-Enkephalin at the Surface of a Hydrated Dimyristoylphosphatidylcholine Bilayer: NMR and MD Simulation

Indira Chandrasekhar,* Wilfred F. van Gunsteren, Giorgia Zandomeneghi, Philip T. F. Williamson, and Beat H. Meier

Contribution from the Laboratory of Physical Chemistry, ETH Zurich, 8093 Zurich, Switzerland

Received July 17, 2005; E-mail: indira@igc.phys.chem.ethz.ch

Abstract: The morphogenic opiate pentapeptide leucine-enkephalin (lenk) in a hydrated dimyristoylphosphatidylcholine (DMPC) bilayer is studied using NMR spectroscopy and molecular dynamics simulation. Contrary to the frequent assumption that the peptide attains a single fixed conformation in the presence of membranes, we find that the lenk molecule is flexible, switching between specific bent conformations. The constraints to the orientation of the aromatic rings that are identified by the NMR experiment are found by the MD simulation to be related to the depth of the peptide in the bilayer. The motion of the N−H vectors of the peptide bonds with respect to the magnetic field direction as observed by MD largely explain the magnitude of the observed residual dipolar coupling (RDC), which are much reduced over the static $^{15}N-^{1}H$ coupling. The measured RDCs are nevertheless significantly larger than the predicted ones, possibly due the absence of long-time motions in the simulations. The conformational behavior of lenk at the DMPC surface is compared to that in the aqueous solution, both in the neutral and in the zwitterionic forms.

1. Introduction

As biological activity of many small peptides is increasingly known to take place in the presence of membranes the interest in elucidating the conformational characteristics of these complex systems at the atomic level has grown. Molecular dynamics (MD) simulation and nuclear magnetic resonance (NMR) spectroscopy, when combined, offer a powerful way to analyze, interpret, and predict the mean conformational and dynamic behavior of biomembrane systems. This article contains an analysis of the peptide leucine-enkephalin (lenk) in the presence of a dimyristoylphosphatidylcholine (DMPC) membrane.

The enkephalins belong to the class of molecules termed as endorphins or endogenous morphines and are implicated in the control of pain, emotion, and a variety of different physiological and immunological functions in mammals.[1−6] There are two naturally occurring enkephalins, whose relative abundance is species dependent.[1,5] They are both pentapeptides that differ only in the identity of the terminal amino acid. Leucine-enkephalin (lenk) contains Leu at the C-terminal end, while methionine-enkephalin (menk) contains Met. From the time of their discovery[1] these pentapeptides have been the subject of intensive conformational study using a variety of spectroscopic and diffraction techniques.[7] A compact bent conformation had been proposed for the monomer, while an extended conformation was suggested to result from a concentration-dependent formation of an antiparallel β sheet dimer.[8] Both forms have been observed through X-ray crystallography.[9−11] Additionally a double-bent form of the peptide has been observed.[12] It is now well established, both experimentally and theoretically, that the conformational behavior of the enkephalins is acutely dependent on solvent[2,13,14] and ionic state.[15−17] In aqueous medium, a conformational equilibrium between different states is indicated over a single preferred conformation.[13]

(1) Huhges, J.; Smith, T. W.; Kosterlitz, H. W.; Fothergill, L. A.; Morgan, B. A.; Morris, H. R. *Nature* **1975**, *258*, 577−579.
(2) Clement-Jones, V.; Besser, G. M. In *The Peptides: Analysis, Synthesis, Biology*; Udenfriend, S., Meienhofer, J., Eds.; Academic Press: New York, 1984; Vol. 6, pp 324−389.
(3) *Opioid Peptides: Medicinal Chemistry*; Rao, R. S., Barnett, G., Hawks, R. L., Eds.; NIDA Research Monograph 69 1986, DHHS Publ. No. (ADM) 90-1454; NIDA: Rockville, MD, 1986.
(4) Schwyzer, R. *Biochemistry* **1986**, *25*, 6335−6342.
(5) *Opioids: Receptors, Analogues, Biological Functions and Therapeutic Applications*; Janecki, T., Ed.; Current Topics in Medicinal Chemistry; Bentham Science Publishers Ltd.: 2004; Vol. 4.
(6) Schiller, P. W. In *The Peptides: Analysis, Synthesis, Biology*; Udenfriend, S., Meienhofer, J., Eds.; Academic Press: New York, 1984; Vol. 6, pp 219−268.
(7) Simantov, R.; Snyder, S. H. *Life Sci.* **1976**, *18*, 781−788.
(8) Khaled, M. A.; Long, M. M.; Thompson, W. D.; Bradley, R. J.; Brown, G. B.; Urry, D. W. *Biochem. Biophys. Res. Commun.* **1977**, *76*, 224−231.
(9) Griffin, G. D.; Smith, J. F. *Science* **1978**, *199*, 1214−1216.
(10) Karle, I. L.; Karle, J.; Mastropaolo, D.; Camerman, A.; Camerman, N. *Acta Crystallogr., Sect. B* **1983**, *39*, 625−637.
(11) Camerman, A.; Mastropaolo, D.; Karle, I.; Karle, J.; Camerman, N. *Nature* **1983**, *306*, 447−450.
(12) Aubry, A.; Birlirakis, N.; Sakarellos-Daitsiotis, M.; Sakarellos, C.; Marraud, M. *Biopolymers* **1989**, *28*, 27−40.
(13) Graham, W. H.; Carter, E. S., II; Hicks, R. P. *Biopolymers* **1992**, *32*, 1755−1764.
(14) van der Spoel, D.; Berendsen, H. J. C. *Biophys. J.* **1997**, *72*, 2032−2041.
(15) Higashijima, T.; Kobayashi, J.; Miyazawa, T. *Eur. J. Biochem.* **1979**, *97*, 43−57.
(16) Aburi, M.; Smith, P. E. *Biopolymers* **2002**, *64*, 177−188.
(17) Abdali, S.; Jensen, M. O.; Bohr, H. *J. Phys.: Condens. Matter* **2003** *15*, S1853−S1860.

As enkephalins and their analogues are among the smallest biologically active peptides, they have been the subject of a number of MD simulation studies. For example, stability of the cyclic analogues of the peptide have been explored[18,19] and the relative merits of different solvent models have been examined with menk as a solute.[20] In water, at neutral pH, lenk is believed to be in the zwitterionic form where both the N and the C termini of the peptide are charged.[15] A recent analysis of Raman spectra at systematically different pH values suggests that a relatively compact lenk structure that involves interaction between the protonated N and deprotonated C termini is stable over a wide pH range.[17] This is corroborated by DFT calculations on the peptide.[21] Simulation studies of neutral and zwitterionic lenk in DMSO and in water, respectively, also suggest that the pentapetide has a tendency to form a compact bent structure through salt bridge formation between the peptide termini[14] although, in this study, which is only 2 ns in length, the influence of the initial conformations persists. More recent MD simulation studies that are 10 ns long also support a bent model with close head to tail arrangement and a 2 → 5 hydrogen bond at neutral pH.[16] Simulations in the presence of different salts or ionic cosolvents, such as NaCl and NH_4Cl,[22−25] detail interactions between the positively charged N terminus and many Cl^- ions. The study suggests that the conformation of the peptide is sensitive to the precise anion that interacts singly with the negatively charged C terminus.[25] In general, simulation studies indicate a bent form for the peptide even in aqueous solution though the details of the bend may vary. MD simulations also show that the dynamics of the side chain torsion angles is significantly affected by the different solvents[14] and by variation in pH.[16]

Spectroscopic observations suggest that the specific conformations of lenk are stabilized by the presence of amphipathic micellar and bilayer systems.[13,26] As the opiate receptors for enkephalins are membrane proteins this leads to the hypothesis that membrane catalysis may be invoked to explain the activity of these highly flexible peptides. The hypothesis implies that the presence of the amphipathic membrane imposes specific structure on the peptide, which may then interact with the appropriate opiate receptor. However, recent studies of the enkephalins associated with bicelles[27−29] suggest conformational diversity even in membranes. Here, we simulate the peptide in both membrane and aqueous environments. The conformational preferences and the mobility of the system are analyzed using experimental NOE and residual dipolar coupling data and simulation data.

2. Materials and Methods

2.1. NMR. 2.1.1. Lenk in Isotropic Bicelles. Sample preparation and NMR experiments are described in the Supporting Information.

2.1.2. Distance Calculations. All cross-peaks in the NOESY spectra are positive, indicating that the bicelle-associated peptide is in the slow-motion limit. A total of 21, 35, and 44 nontrivial cross-peaks were observed in the NOESY spectra with mixing times of 100, 200, and 300 ms, respectively. The Tyr1 aromatic protons Hδ1/Hδ2 and Hϵ1/Hϵ2, Tyr1 Hβ/Hβ′, Gly2 Hα/Hα′, Gly3 Hα/Hα′, Phe4 aromatic protons Hδ1/Hδ2 and Hϵ1/Hϵ2, Leu5 Hβ/Hβ′ and Hδ/Hδ′ are not resolved. The interproton distances have been calculated by assuming a single correlation time for the whole molecule and, in initial rate approximation, the distance r between two protons is related to the corresponding cross-peak intensity I by the relationship $r^{-1} = A\sqrt[6]{I}$. Here A is the mixing-time-dependent constant for all the pairs of protons, which was determined using cross-peak Tyr1 Hδ1/Hδ2 → Hϵ1/Hϵ2 corresponding to an internuclear distance of 0.25 nm. The uncertainty in the distance, Δr, was calculated as the maximum deviation from the average distance for the three NOESY spectra at different mixing times. Because the water suppression applied in the experiments reduces the signal intensity of the amide exchangeable proton resonances, the Δr for these protons is assumed to be equal to the difference between the distances calculated from the nonnormalized and the normalized cross-peak intensities. Distances corresponding to weak but detectable cross-peaks such that $r > 0.5$ nm were set at 0.6 nm with $\Delta r = 0.1$ nm.

2.1.3. Simulated Annealing. The simulated annealing (SA) to obtain NMR model structures and the subsequent analysis of these structures were carried out using the Insight II (version 97.2)[31] program package (Accelrys, CA) employing the consistent valence force field (CVFF)[32] in vacuo. In the Supporting Information we describe the SA protocol for the determination of the lenk conformers with the lowest target function consistent with the 44 distance constraints derived from the NOESY spectra, the peptide torsion angles (restrained in the trans conformation), and the 2 dihedral restraints ϕ from the $^3J_{NH-H\alpha}$ couplings of Phe4 and Leu5, both 7.92 Hz.[45]

2.1.4. ^{15}N Fully Labeled Lenk in Oriented Bicelles. Sample preparation and NMR experiments are reported in ref 30. Details are given in the Supporting Information along with a description of the determination of the ^{13}C residual chemical-shielding anisotropy (RCSA) of the aromatic carbons.

(18) Hruby, V. J.; Kao, L.-F.; Pettitt, B. M.; Karplus, M. *J. Am. Chem. Soc.* **1988**, *110*, 3351−3359.
(19) Wang, Y.; Kuczera, K. *J. Phys. Chem.* **1996**, *100*, 2555−2563.
(20) Shen, M.-Y.; Freed, K. F. *Biophys. J.* **2002**, *82*, 1791−1808.
(21) Abdali, S.; Refstrup, P.; Faurskov Nielsen, O.; Bohr, H. *Biopolymers* **2003**, *72*, 318−328.
(22) Smith, P. E.; Pettitt, B. M. *J. Am. Chem. Soc.* **1991**, *113*, 6029−6037.
(23) Smith, P. E.; Dang, L. X.; Pettitt, B. M. *J. Am. Chem. Soc.* **1991**, *113*, 67−73.
(24) Smith, P. E.; Marlow, G. E.; Pettitt, B. M. *J. Am. Chem. Soc.* **1993**, *115*, 7493−7498.
(25) Marlow, G. E.; Pettitt, M. B. *Biopolymers* **2003**, *68*, 192−209.
(26) Takeuchi, H.; Obtsuka, Y.; Harada, I. *J. Am. Chem. Soc.* **1992**, *114*, 5321−5328.
(27) Zandomeneghi, G. Ph.D. Thesis, 15091, ETH-Zürich, Zürich, Switzerland, 2003.
(28) Marcotte, I.; Dufourc, E. J.; Ouellet, M.; Auger, M. *Biophys. J.* **2003**, *85*, 328−339.
(29) Marcotte, I.; Separovic, F.; Auger, M.; Gagné, S. M. *Biophys. J.* **2004**, *86*, 1587−1600.
(30) Zandomeneghi, G.; Meier, B. H. *J. Biomol. NMR* **2004**, *30*, 303−309.
(31) *Insight II*; NMRchitect; Accelrys: San Diego, CA, 2000.
(32) Dauber-Osguthorpe, P.; Roberts, V. A.; Osguthorpe, D. J.; Wolff, J.; Genest, M.; Hagler, A. T. *Proteins: Struct., Funct., Genet.* **1988**, *4*, 31−47.
(33) Schuler, L. D.; Daura, X.; van Gunsteren, W. F. *J. Comput. Chem.* **2001**, *22*, 1205−1218.
(34) Berendsen, H. J. C.; Postma, J. P. M.; van Gunsteren, W. F.; Hermans, J. In *Interaction Models for Water in Relation to Protein Hydration*; Pullman, B., Ed.; Reidel: Dordrecht, The Netherlands, 1981; pp 331−342.
(35) Chandrasekhar, I.; Kastenholz, M.; Lins, R. D.; Oostenbrink, C.; Schuler, L. D.; Tieleman, D. P.; van Gunsteren, W. F. *Eur. Biophys. J.* **2003**, *38*, 67−77.
(36) van Gunsteren, W. F.; Billeter, S. R.; Eising, A. A.; Hünenberger, P. H.; Krüger, P.; Mark, A. E.; Scott, W. R. P.; Tironi, I. G. *Biomolecular Simulation: The GROMOS96 Manual and User Guide*; vdf Hochschulverlag AG an der ETH Zürich and BIOMOS b v: Zürich, Groningen, 1996.
(37) Scott, W. R. P.; Hünenberger, P. H.; Tironi, I. G.; Mark, A. E.; Billeter, S. R.; Fennen, J.; Torda, A. E.; Huber, T.; Krüger, P.; van Gunsteren, W. F. *J. Phys. Chem. A* **1999**, *102*, 3596−3607.
(38) Berendsen, H. J. C.; Postma, J. P. M.; van Gunsteren, W. F.; DiNola, A.; Haak, J. R. *J. Chem. Phys.* **1984**, *81*, 3684−3690.
(39) Ryckaert, J. P.; Ciccotti, G.; Berendsen, H. J. C. *J. Comput. Phys.* **1977**, *23*, 327−341.
(40) Tironi, I. G.; Sperb, R.; Smith, P. E.; van Gunsteren, W. F. *J. Chem. Phys.* **1995**, *102*, 5451−5459.
(41) Laskowski, R. A.; MacArthur, M. W.; Moss, D. S.; Thornton, J. M. *Proteins* **1993**, *12*, 345−364.
(42) Vold, R. R.; Prosser, R. S.; Deese, A. J. *J. Biomol. NMR* **1997**, *9*, 329−335.
(43) Chou, J. J.; Kaufman, J. D.; Stahl, S. J.; Wingfield, P. T.; Bax, A. *J. Am. Chem. Soc.* **2002**, *124*, 2450−2451.
(44) Glover, K. J.; Whiles, J. A.; Wu, G.; Yu, N.; Deems, R.; Struppe, J. O.; Stark, R. E.; Komives, E. A.; Vold, R. R. *Biophys. J.* **2001**, *81*, 2163−2171.
(45) Karplus, M. *J. Chem. Phys.* **1959**, *30*, 11−15.

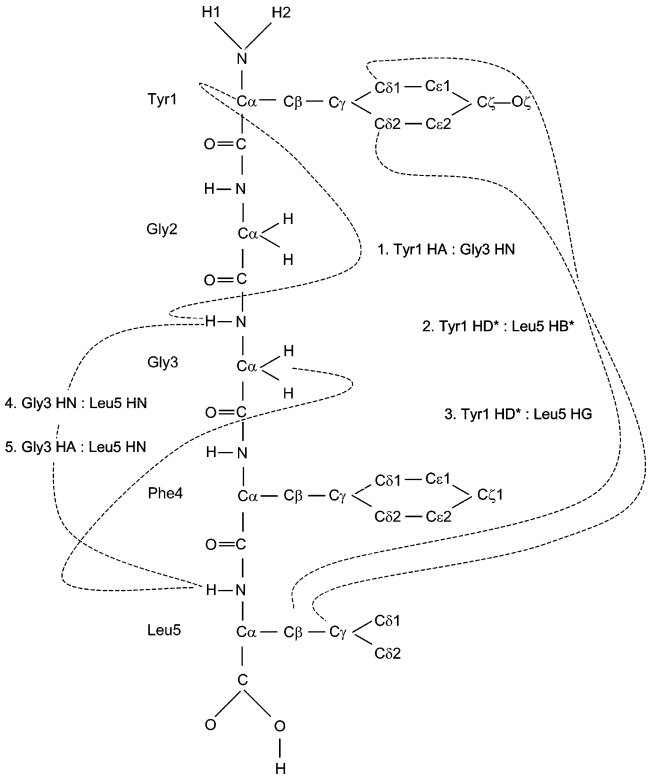

Figure 1. Schematic of the lenk molecule. Measured longer-range NOE distance bounds indicated by the dashed lines are numbered as in Table 2.

2.2. Molecular Dynamics Simulations. Six simulations of the peptide (Figure 1), each 50 ns in length, were generated. In four of the simulations the neutral (lnkn) and in the remaining two cases the zwitterionic (lnkz) forms of the molecule were used. The peptide was placed either in a water box or at the surface of a hydrated DMPC bilayer as described below. In all cases the peptide was modeled using the GROMOS96 45A3 force field.[33] The simple point charge (SPC) model[34] was used to represent the water molecules. One of the conformations derived from the NMR data of lenk at the surface of oriented DMPC/DHPC bicelles was used as the initial structure. Coordinates for the hydrated DMPC bilayer were obtained after 5 ns of simulation using the model and setup described in ref 35. All simulations were carried out using the GROMOS96 simulation package.[36,37] The simulations were run at the experimental temperature of 308 K. The temperature of the lipids and the water molecules were separately coupled to a temperature bath with a coupling time of 0.1 ps.[38] In all cases, anisotropic pressure coupling was used where pressure was calculated using a molecular virial.[38] Bond lengths were constrained to ideal values using the SHAKE algorithm[39] with a geometric tolerance of 10^{-4}. The time step for the leapfrog integration scheme was set to 2 fs. The nonbonded interactions were treated using the triple-range cutoff scheme.[40] The specifics of the six simulations are described below and are summarized in Table 1.

2.2.1. Lenk in Water. In the simulations in water, the peptide in the two ionic forms (lnkn and lnkz) in the bent conformation of the NMR model structure was placed at the center of a truncated octahedron box, with the minimum distance from any peptide atom to any box wall of 1.4 nm. In both the lnkn−H_2O system and in the lnkz−H_2O system the box length was 4.1 nm. The boxes were filled with SPC water molecules, and all water molecules within 0.3 nm of a non-hydrogen peptide atom were removed. The lnkn−H_2O system contains 1114 water molecules, and the lnkz−H_2O system contains 1120 water molecules. Truncated octahedron boundary conditions were applied. The systems were minimized using steepest-descent minimization while keeping the position of the peptide atoms restrained. Following this a steepest-descent minimization of the model was performed without restraints to eliminate residual strain. The energy minimization was terminated when the energy change per step was smaller than 0.1 kJ mol^{-1}. The MD simulations of each of the systems in water were run for 50 ns.

2.2.2. Lenk at the Surface of a Hydrated DMPC Bilayer. The lenk molecule in the bent NMR conformation was placed by visual means at the surface of the 8 × 8 DMPC bilayer so that it was oriented with the curve of the bend pointing away from the membrane surface and the two aromatic rings pointing toward the membrane, as suggested by the NMR experiment.[27] Although the fraction of lipid-associated lenk is evaluated by monitoring the ^{13}C isotropic chemical shifts in isotropic bicelle solutions as a function of the concentration ratio, this number is subject to error as the differences in chemical shifts are sensitive to many factors. Further, as this number is close to 1 (see section 3.1.3), we confine ourselves to a single enkephalin molecule and do not address issues that may arise either from aggregation or from exchange of the lenk molecule between aqueous and membrane environments. The 8 × 8 bilayer that has been used as a standard in the evaluation of the GROMOS96 force field and simulation parameters[35] was used to model the membrane. The hydrated bilayer consists of 5888 DMPC atoms (46 GROMOS96 atoms per DMPC molecule) and 3655 water molecules. Rectangular boundary conditions are applied. Both the neutral and zwitterionic forms of the lenk molecule displaced 23 waters resulting in 28.4 waters per DMPC molecule, consistent with full hydration. As in the case of lenk in water, the peptide was first positionally restrained by a harmonic force which was later released and a steepest-descent minimization performed to relieve short distance contacts. The water and DMPC headgroups could thus adjust to the presence of the pentapeptide. The lnkn−DMPC membrane system was simulated in three different ways. The first, without NMR distance restraints applied (lnkn−DMPC), was for 50 ns. The second, in which the NOE distance restraints were applied during the simulation (lnkn−$DMPC_{NOE}$), was terminated after 20 ns. The third simulation, in which the NMR restraints were released after 5 ns (lnkn−$DMPC_{rel}$), was run up to 50 ns. The system with the zwitterionic form of the peptide (lnkz−DMPC) was simulated without restraints for 50 ns.

2.2.3. NOE Distances in Simulation: Calculation and Restraining. During the lnkn−$DMPC_{NOE}$ simulation all 44 interproton distances (see Table S3 in the Supporting Information) were restrained using an attractive harmonic potential function with a force constant of 10^3 kJ mol^{-1} nm^{-2} for distances between the NOE upper bounds and the NOE bounds plus 0.1 nm and a linear potential function for distances exceeding the NOE bounds by 0.1 nm. Thus, the experimentally determined orientation of the ring and the compactness of the structures were maintained during simulation. The hydrogen atoms that form part of united carbon atoms that are involved in the distance bounds were explicitly constructed as described in ref 36. In this case no pseudoatom corrections needed to be applied. The aromatic protons are experimentally indistinguishable, as discussed above. We represent the NOE distance bound involving the aromatic protons as two bounds, one involving the two Hδ protons and the other the two Hϵ protons.

For the analysis, the interproton distances were calculated for the structures in the six MD trajectories and were averaged using r^{-6} averaging. In the case of the aromatic rings, we calculate the distance from the Hδ and Hϵ protons and report their mean. The r^{-6}-averaged interproton distances are also presented as distance upper bound violations, i.e., as distances averaged over the ensemble minus the corresponding NMR upper distance bound. The difference can be positive or negative, the latter case implying that in the MD simulations the interproton distance is on average shorter than the upper bound derived from the NMR experiment.

2.2.4. Analysis of the Structures from Simulation. Structures of the peptide were extracted from the trajectories at 0.01 ns intervals for analysis. For every pair of structures a least-squares translational and rotational fit was performed using the backbone (N, Cα, C) atoms of Gly2, Gly3, and Phe4. Thus in performing the fit, the backbone atoms

Table 1. Summary of the Six MD Simulations of Leu-Enkephalin

environment	electronic form	simulation	NOE distance restraints	length of the simulation (ns)	color in figures
water	neutral	lnkn−H_2O	none	50	blue
	zwitterionic	lnkz−H_2O	none	50	red
at surface of hydrated DMPC bilayer	neutral	lnkn−DMPC	none	50	blue
	zwitterionic	lnkz−DMPC	none	50	red
	neutral	lnkn−$DMPC_{NOE}$	applied	20	indigo
	neutral	lnkn−$DMPC_{rel}$	released after 5 ns of lnkn−$DMPC_{NOE}$	45	magenta

of only the central three residues are considered. At each time point the atom-positional root-mean-square deviation (rmsd) of the structure from the initial NMR model structure was evaluated. The program PROCHECK[41] was used to evaluate the secondary structural element present at the five residues from the value of the respective backbone dihedral angles at each time point.

3. Results and Discussion

3.1. Structural Information from NMR Experiments. 3.1.1. ^{1}H NMR Experiments on Lenk/Isotropic Bicelles. Lipid systems with [DMPC]/[DHPC] < 2 do not orient in the magnetic field and provide isotropic NMR spectra.[42,43] Such bicelle systems are supposed to have the same morphology and lipid organization as bicelles with larger [DMPC]/[DHPC], which self-orient in the magnetic field.[44] The assignment of the ^{1}H NMR signals of lenk in a bicelle sample with [DMPC]/[DHPC] = 0.5 and [lipids]/[lenk] = 13 is shown in Table S1 in the Supporting Information.

The conformation of bicelle-associated lenk in isotropic bicelles has been studied using interproton distance constraints obtained from ^{1}H NOESY NMR experiments (Table S3 in the Supporting Information). A group of 9 structures was selected out of the 20 structures with lowest target function value, after exclusion of the conformations with largest distance-constraint violations. The nine structures can be grouped in two families of seven and two structures, which differ from each other in the torsion angle ψ of the Gly3 residue. The group of seven conformations is characterized by $\psi = -90° \pm 2°$ and the other two structures by $\psi = 90° \pm 1°$ (Table S2 in the Supporting Information). The larger group adopts a 5 → 2 β turn, with the average distance between the Cα atoms of residues Gly2 and Leu5 of 0.6 nm (see Figure 4). This conformation, shown in red in the Table of Contents figure with conformations from simulation superimposed upon it, is similar to the conformation of lenk determined in SDS micelles[46] and to [D-Ala-2]-lenk associated to mixed vesicles of dipalmitoylglycerophosphocholine and dilauroylglycero-phospho-DL-serine.[47]

3.1.2. ^{1}H and ^{13}C NMR Experiments on Lenk/Oriented Bicelles. Information about the orientation of the aromatic rings in Tyr1 and Phe4 with respect to the bicelle normal in lipid-associated lenk can be derived from the ^{13}C RCSAs and the ^{1}H−^{1}H RDCs within the rings. In particular, the ^{1}H−^{1}H RDC between the protons ^{1}Hδ1/ϵ1 and ^{1}Hδ2/ϵ2 of the Tyr1 side chain has been determined and can be related to the average P_2 associated with the angle between the vector ^{1}Hδ1−^{1}Hϵ1 (or ^{1}Hδ2−^{1}Hϵ2) and the bicelle normal.[52] The ^{13}C RCSAs can be determined from the comparison of the ^{13}C chemical shift of lenk in a static sample, where the bicelles are oriented with the director perpendicular to the magnetic field, and in a sample spun at the magic angle, where the system provides isotropic NMR spectra. The orientation of the rings cannot be fully determined (Supporting Information), but the range for the angle β between the axis Cγ−Cζ in the aromatic ring and the bilayer normal is $56° \le \beta \le 96°$ for the Tyr1 ring and $46° \le \beta \le 81°$ and $99° \le \beta \le 135°$ for Phe4 (indicated in Figure 5). The case of Tyr1 is better defined as the ^{1}H−^{1}H RDCs are unresolved in the case of Phe4.

3.1.3. ^{15}N NMR Experiments on Lenk/Oriented Bicelles. ^{1}H−^{15}N residual dipolar couplings (RDC) of lenk associated to oriented bicelles with [DMPC]/[DHPC] = 3 have been determined and are listed in Table 3. The RDC values depend on the angle between the ^{1}H−^{15}N bond and the normal to the phospholipids bilayer, Θ, according to the relation:

$$\mathrm{RDC} = -0.5 f S_{\mathrm{Bic}} D P_2(\cos \Theta) \qquad (1)$$

where $P_2(\cos\Theta) = (3\cos^2\Theta - 1)/2$ is the second-order Legendre polynomial. The factor −0.5 is the expected reduction of the dipolar interaction for fast rotation of the peptide around the bicelle normal.[27] The factor f represents the molar fraction of bicelle-associated lenk, where it is assumed that lenk is in equilibrium between an oriented, lipid-associated form and a free form which tumbles quasi-isotropically.[48−50] The value of f was determined from the positions of the ^{13}C chemical shifts of lenk in isotropic bicelles ([DMPC]/[DHPC] = 0.5), measured as function of the concentration ratio ([DMPC] + [DHPC])/[lenk].[48] For the system ([DMPC] + [DHPC])/[lenk] = 13, f = 0.9, a value consistent with literature data.[49,50] $S_{\mathrm{Bic}} = 0.65$ is the bicelle order parameter that accounts for the additional motions of the bicelles relative to those of DMPC vesicles and can be determined from the comparison of the ^{31}P chemical shift of DMPC in bicelles and vesicles.[50,51] D is the dipolar coupling constant in frequency units for ^{1}H−^{15}N in a peptide bond and is assumed to be 11.48 kHz, corresponding to a static N−H with a distance of 1.02 A. The dimensionless $P_2(\cos\Theta)$ values are the only unknown on the right-hand side in the equation defining the RDCs, and the corresponding values are listed in Table 3 and indicated in Figure 8.

3.2. Results from MD Simulation. 3.2.1. Backbone Conformation and Motion. The conformational behavior of the two electronic forms of the peptide, the neutral (lnkn) and zwitterionic (lnkz), in different simulations is summarized in Figure 2. In Figure 2a the secondary structural elements at each

(46) Picone, D.; D'Ursi, A.; Motta, A.; Tancredi, T.; Temussi, P. A. *Eur. J. Biochem.* **1990**, *192*, 433−439.
(47) Milon, A.; Miyazawa, T.; Higashijima, T. *Biochemistry* **1990**, *29*, 65−75.
(48) Deber, C. M.; Behnam, B. A. *Proc. Natl. Acad. Sci. U.S.A.* **1984**, *81*, 61−65.
(49) Sanders, C. R.; Landis, G. C. *Biochemistry* **1995**, *34*, 4030−4040.
(50) Sanders, C. R.; Landis, G. C. *J. Am. Chem. Soc.* **1994**, *116*, 6470−6471.
(51) Zandomeneghi, G.; Tomaselli, M.; Williamson, P. T. F.; Meier, B. H. *J. Biomol. NMR* **2003**, *25*, 113−123.
(52) Zandomeneghi, G.; Williamson, P. T. F.; Hunkeler, A.; Meier, B. H. *J. Biomol. NMR* **2003**, *25*, 125−132.

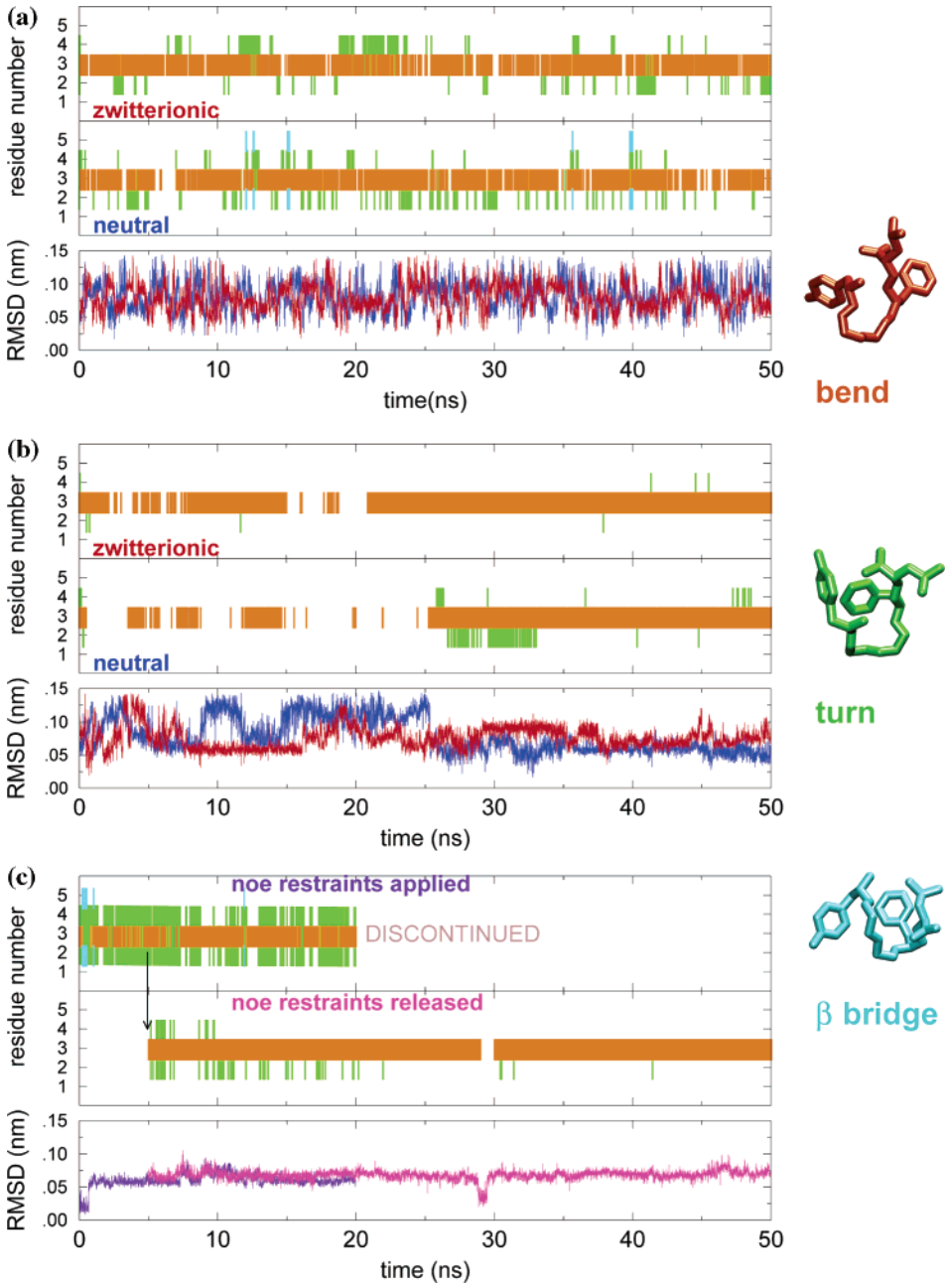

Figure 2. Top and middle panels depict the secondary structure at each residue with time. (a) In water: top panel, zwitterionic lnkz−H_2O; middle panel, neutral, lnkn−H_2O. (b) At the surface of a DMPC bilayer: top panel, zwitterionic lnkz−DMPC; middle panel, neutral lnkn−DMPC. (c) At the surface of a DMPC bilayer: top panel, lnkn−$DMPC_{NOE}$; middle panel, lnkn−$DMPC_{rel}$. In all cases the bend is shown in orange, the turn in green, and the β turn in cyan. Typical backbone structures are shown alongside in the corresponding colors. The bottom panel shows the backbone (residues 2−4) atom-positional root-mean-square deviation (rmsd) from the initial NMR model structure using the following symbols. (a) In water: lnkn, blue line; lnkz, red line. (b) At the surface of a DMPC bilayer: lnkn, blue line; lnkz, red line. (c) At the surface of a DMPC bilayer: lnkn with NOE restraints applied, indigo line; lnkn with NOE restraints released after 5 ns, magenta line.

residue in the simulations with the neutral (middle panel) and zwitterionic (top panel) peptide in water are seen. Figure 2b shows the behavior of the neutral (middle panel) and zwitterionic (top panel) peptide at the surface of a DMPC membrane, and Figure 2c shows the simulations with NOE distance restraints applied (top panel) and released (middle panel). The presence of a secondary structural element at each residue is indicated by a vertical line whose color code is detailed in the figure caption. In each part of Figure 2a−c the bottom panel shows the rmsd of the peptide backbone from the initial NMR structure. There is no significant difference in the behavior of the neutral and zwitterionic forms in the different simulations. In water (Figure 2a), the peptide conformation fluctuates rapidly as evidenced by the rmsd. Although a bend is present at residue 3 and turns are identified at residues Gly2 and Phe4, there is no dominant stable conformation. At the surface of the DMPC bilayer, however, the peptide remains stable in the bent conformation for periods of over 20 ns (Figure 2, parts b and c). The bend at residue 3 dominates for 60% of the time in the neutral form and 75% of the time in the zwitterionic form as evaluated using the DSSP program.[53] In the neutral form of the peptide, residues Gly2 and Phe4 adopt turn conformations that

(53) Kabsch, W.; Sanders, C. *Biopolymers* **1983**, *22*, 2577−2637.

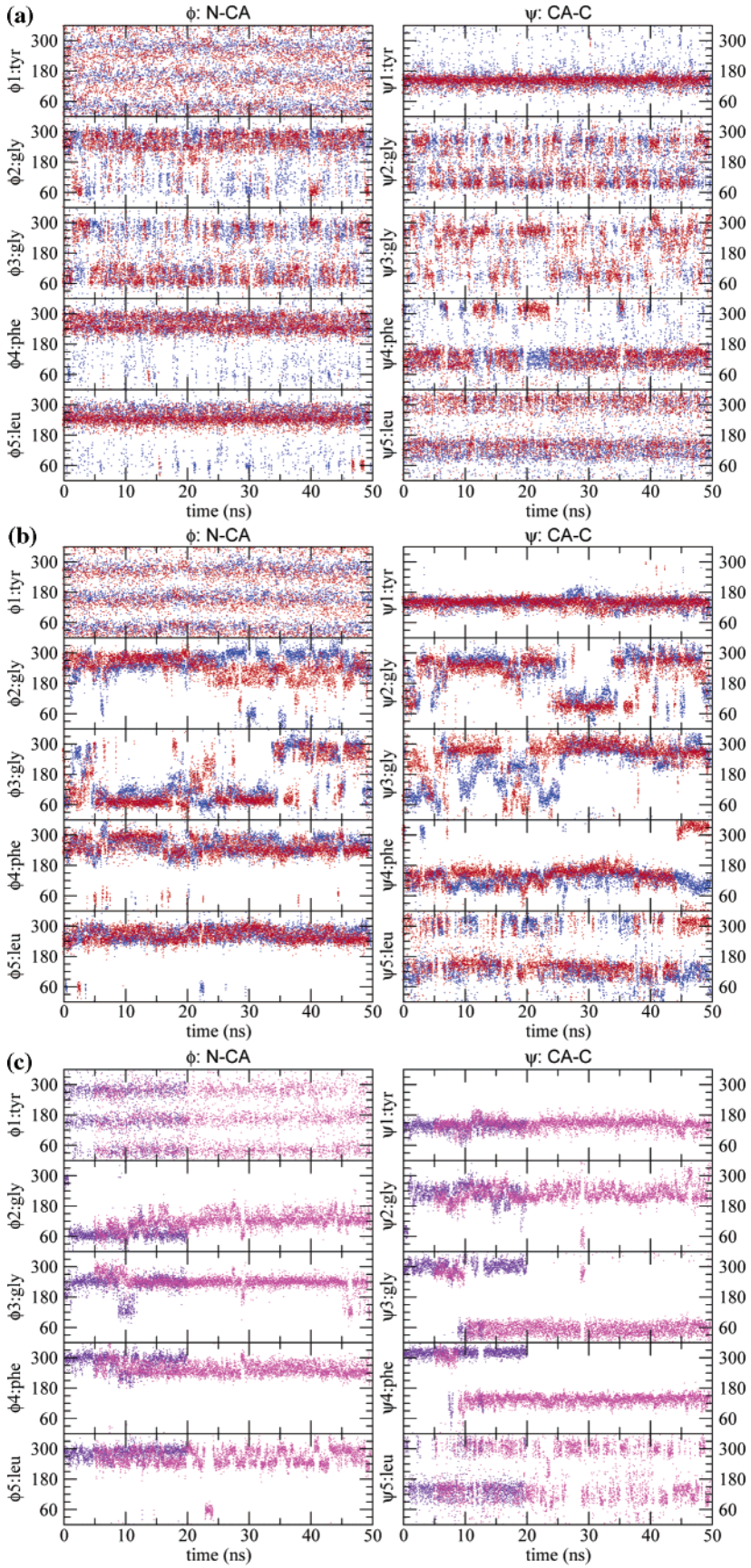

Figure 3. Time behavior of the five ϕ and ψ backbone dihedral angles in the peptide. (a) In water: lnkn−H_2O, blue dots; lnkz−H_2O, red dots. (b) At the surface of a DMPC bilayer: lnkn−DMPC, blue dots; lnkz−DMPC, red dots. (c) At the surface of a DMPC bilayer: lnkn−$DMPC_{NOE}$, indigo dots; lnkn−$DMPC_{rel}$, magenta dots.

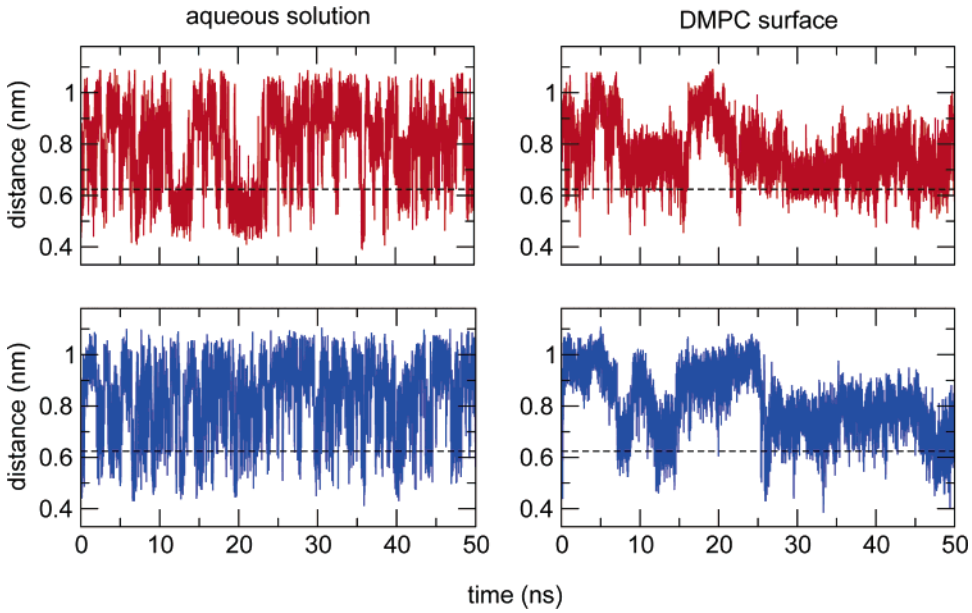

Figure 4. Distance from the Cα atom of Gly2 to that of Leu 5 as a function of time. The results from the lnkn (blue) and lnkz (red) simulations in water are in the left panels, and those from the simulation at the DMPC surface are on the right. The horizontal dashed lines represent the experimental value determined for lenk at the membrane surface.

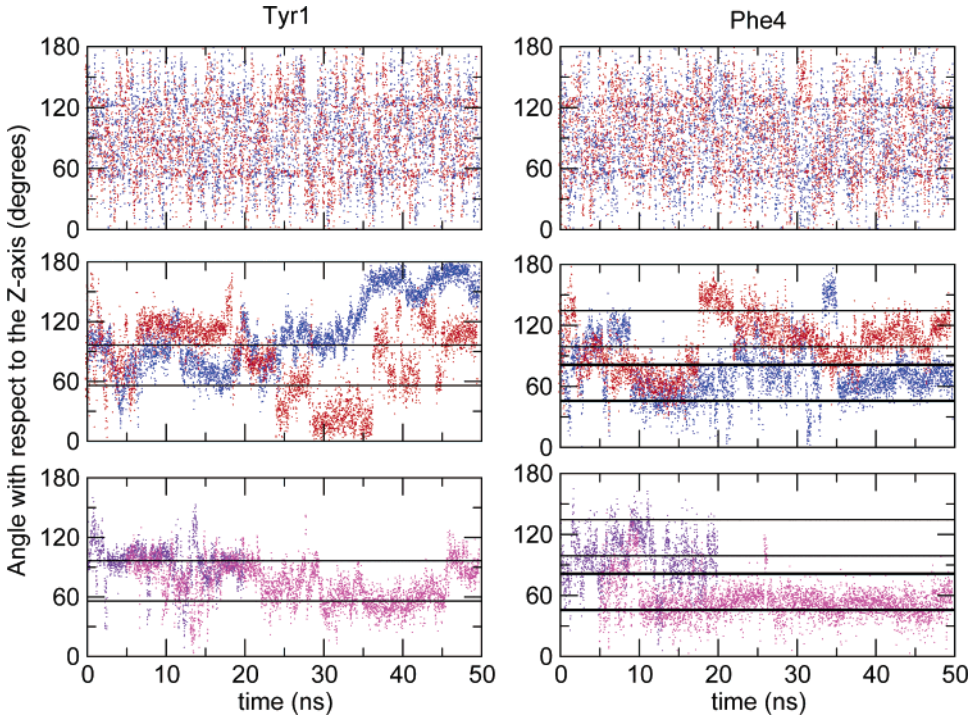

Figure 5. Time behavior of the angle between the vectors defined as the line from the Cγ to the Cζ atom of the aromatic rings of Tyr1 (left column) and Phe4 (right column) with respect to the *Z*-axis, which is coincident with the bilayer normal. Top panel, in water: lnkn−H_2O (blue dots), lnkz−H_2O (red dots). Middle panel, at the surface of a DMPC bilayer: lnkn−DMPC (blue dots) and lnkz−DMPC (red dots). Bottom panel, at the surface of a DMPC bilayer: lnkn−$DMPC_{NOE}$ (indigo dots), lnkn−$DMPC_{rel}$ (magenta dots). The limits derived from the NMR experiment of lenk at the membrane surface are shown as horizontal black lines.

are more stable in the simulations where NOE distance restraints are applied. On release of the restraints the peptide adopts a conformation very similar to that in the unrestrained simulation, with a bend at residue 3 being the strongest secondary structural feature.

In Figure 3a−c the behavior of the ϕ and ψ angles of the five residues of the peptide are shown in (a) water in neutral (blue) and zwitterionic (red) forms, (b) at the DMPC surface in neutral (blue) and zwitterionic (red) forms, and (c) at the DMPC surface on application (indigo) and release (magenta) of the NOE distance restraints. The transitions of the ϕ angle at the N terminus and the ψ angle at the C terminus are included for completeness. The dihedral angles of the bulky residues, Tyr1, Phe4, and Leu5 adopt similar skewed or staggered conformations in all the simulations, whereas the glycine dihedral angles show much less evidence of pronounced distributions, fluctuating primarily between staggered or skewed conformations. At the DMPC surface, the bend at Gly3 occurs when the ψ dihedral

Table 2. Experimental NOE Distance Bounds in nm and the Calculated r^{-6}-Averaged Value from the Six Leu-Enkephalin Simulations, Where r Is the Interproton Distance

number[a]	1	2	3	4	5
NOE pair	Tyr1 HA | Gly3 HN	Tyr1 HD* | Leu5 HB* [b]	Tyr1 HD* | Leu5 HG [b]	Gly3 HN | Leu5 HN	Gly3 HA* | Leu5 HN [b]
NOE upper bound	0.52	0.70	0.70	0.36	0.45
lnkn−H_2O[c]	0.53	0.62	0.59	0.55	0.52
lnkz−H_2O[c]	0.52	0.55	0.58	0.50	0.51
lnkn−DMPC[c]	0.51	0.68	0.57	0.60	0.55
lnkz−DMPC[c]	0.52	0.66	0.57	0.52	0.55
lnkn−$DMPC_{NOE}$[c]	0.56	0.51	0.61	0.31	0.46
lnkn−$DMPC_{rel}$[c]	0.55	0.88	0.99	0.54	0.57

[a] Numbers correspond to the NOE pairs indicated in Figure 1. [b] The asterisk indicates that the two protons are experimentally indistinguishable and a pseudoatom distance is reported. The calculated values from simulation are the mean of the value from each of the two protons. [c] Names correspond to systems described in Table 1.

Table 3. Experimental Residual $^1H-^{15}N$ Dipolar Couplings and the Corresponding P_2 Legendre Functions of the Angles, θ, that the N−H Vectors Make with the Magnetic Field Direction of Lenk in Oriented Bicelles at 313 K and the Average of the Calculated P_2 Legendre Functions of the Angles, θ, that the N−H Vectors Make with the $X-Y$ (Bilayer) Plane in the MD Simulations[a]

	NMR experiment		MD simulation $P_2(\cos\theta)$	
residue	RDC/Hz	$P_2(\cos\theta)$	neutral	zwitterionic
Gly2	−5 (2)	0.00	−0.04(0.01)	0.00(0.01)
Gly3	198 (9)	−0.06	−0.16(0.01)	−0.05(0.01)
Phe4	73 (5)	−0.02	−0.10(0.01)	−0.15(0.01)
Leu5	240 (20)	−0.07	−0.15(0.01)	−0.06(0.01)

[a] Shown in parentheses in column 1 is the error in determining the experimental values. The estimated error evaluated from block averages of the root-mean-square deviation for the value from simulations is shown in parentheses in columns 5 and 6 for the respective cases.

angle is in the staggered conformation. In water, there is considerable and rapid torsional motion at the glycines. In contrast, at the DMPC surface, dihedral-angle transitions are much less frequent. In the simulations with the NOE distance restraints there are markedly fewer dihedral-angle transitions than in the unrestrained simulations. This is not unexpected as particular distances are continuously restrained. Release of the restraints results in a transition at the ψ angle of Gly3, which is compensated for by a corresponding transition in the ψ angle of Phe4. In this simulation the bend remains stable over almost the entire trajectory (Figure 2c). Corresponding Ramachandran plots are shown in the Supporting Information.

The approximate distance between the Cα atoms of residues Gly2 and Leu5 in the NMR model structure is 0.6 nm (see section 3.1.1). The value measured in the simulations in water (left panels) and at the DMPC surface (right panels) for the neutral (blue) and zwitterionic (red) forms of lenk are shown in Figure 4. In the water simulations the mean end-to-end distance is 0.8 nm for both neutral and zwitterionic forms of the peptide. At the membrane surface the value fluctuates between 0.6 nm when there is a bend at Gly3 (Figure 1) and 1.0 nm when there is no bend. In a fully extended form the Cα−Cα distance between residues Gly2 and Leu5 is 1.1 nm.

Our results on the conformation of lenk support a compact bent form of the peptide. The lenk molecule is unstable in water, undergoing rapid conformational transitions. At the surface of the DMPC bilayer, however, compact conformations, stable over periods of nanoseconds, are observed. These conformations are dominated by a bend at Gly3 (Figure 2). When the bend is present the other backbone dihedral angles may undergo complementary transitions that do not disrupt the secondary structure. In the neutral form of the peptide, the bend at Gly3 is disrupted in the first 25 ns by transitions at the ψ dihedral angle of Gly3 (Figure 3b). This dihedral angle is different in the two different groups of NMR model structures.

3.2.2. Orientation of the Rings. The angle, β, that the ring vector, defined as the vector between the ring atoms Cγ and Cζ, makes with the Z-axis that is coincident with the normal to the bilayer is shown in Figure 5 for Tyr1 (left panels) and Phe4 (right panels). The results from the simulations of the neutral (blue) and the zwitterionic (red) form of the peptide in water are shown in the top panel, at the DMPC surface in the middle panel, and of the neutral peptide simulated with NOE restraints applied (indigo) and released (magenta) in the bottom panel. The limits of the range of β determined by experiment (section 3.1.3) are indicated as described in the figure caption. As anticipated, the ring vectors in water show no preferred orientation. At the membrane surface, however, the mobility of the rings is clearly restricted. In the simulations where the NOE distance restraints are applied and released (bottom panels) the orientation of the ring vectors does not fluctuate much outside the experimental range. The same is true of the Phe4 ring vector in the unrestrained simulations. The Tyr1 ring, however, reorients at about 35 ns in the neutral peptide in the unrestrained simulation so as to be antiparallel to the Z-axis.

To analyze the change in the orientation of Tyr1, we calculated the side chain dihedral angles χ_1 and χ_2 that orient the ring with respect to the peptide backbone (see the Supporting Information for plots). The dihedral angles about the bonds between Cα−Cβ and Cβ−Cγ do not change at 35 ns. However, backbone dihedrals ψ of Gly2 and ϕ of Gly3 undergo transitions at this time point (Figure 3). The reorientation that causes the ring vector to align along the Z-axis is related to a conformational transition in the peptide.

Figure 6 shows the projection along the Z-axis of the five Cα atoms as a function of time. The position of the central atom, C2, of the glycerol backbone, the bridge between the hydrophilic headgroup and the hydrophobic tails of the DMPC molecule, is also plotted at 1 ns intervals. The normalized density distribution of the C2 atoms along the bilayer normal for each of the two layers is shown on the right. The relative positions of the Cα atoms with respect to the C2 atoms indicate the depth of penetration of the molecule in the bilayer. The ordinate of the plot, along which the direction of the bilayer normal is oriented, spans 6.89 nm, the dimension of the initial simulation box in the z direction. The results from the simulation of the zwitterionic form of lenk are shown in the top panel and those from the neutral form in the bottom panel. The five Cα atoms are represented using five different colors as detailed in the figure caption. Between 25 and 35 ns, there is a spreading or a fanning out of the Cα positions accompanied by a shift of the atoms toward the aqueous polar region. It should be noted that this shift implies a reorientation of the peptide at the membrane surface rather than its departure into the water layer. The shift does not cause a disruption of the bend at Gly3 (Figure 2). This period is characterized by a change in the Gly2 ψ angle from 270/300° to 90/60° (Figure 3) accompanied by the

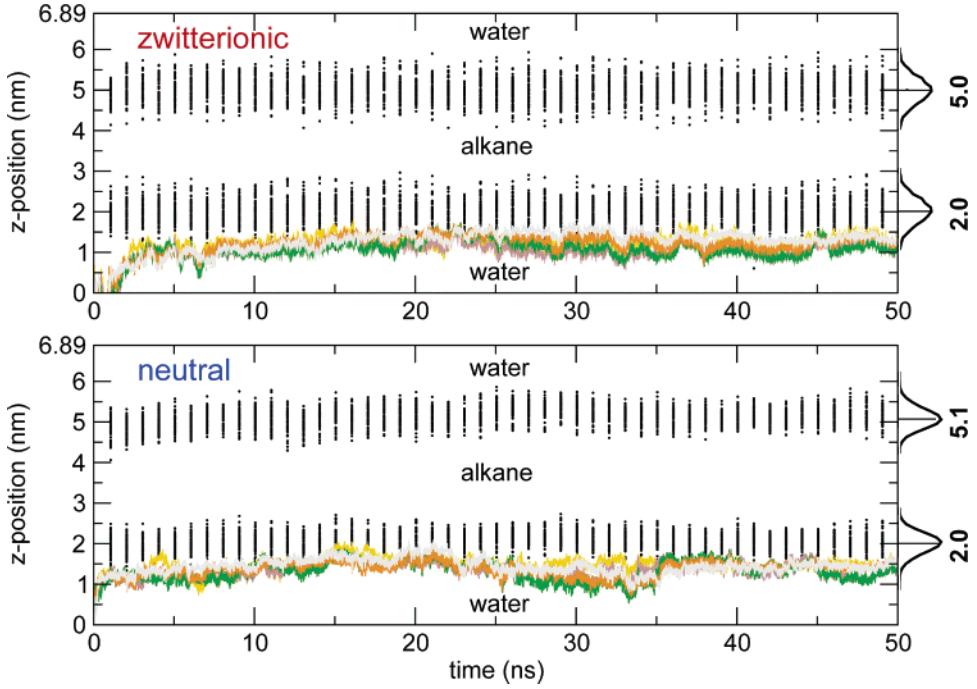

Figure 6. Depth into the bilayer or position along the *Z*-axis (parallel to the bilayer normal) of the Cα atoms from simulations of the neutral form (lnkn) in the bottom panel and the zwitterionic form (lnkz) in the top panel: Tyr1 (yellow), Gly2 (brown), Gly3 (dark green), Phe4 (orange), and Leu5 (grey). An initial box-size of 6.89 nm was used along the ordinate. The positions of the glyceride atoms, C2, of the 64 DMPC molecules in each layer of the bilayer at intervals of 10 ns are shown as black dots. The relative positions of the alkane and water layers in each case are indicated. The density distribution of glyceride atoms, C2, along the *Z*-axis in each of the layers, aligned with respect to the position in *Z* of the distribution peak (indicated by a labeled horizontal black line) is shown on the right-hand side.

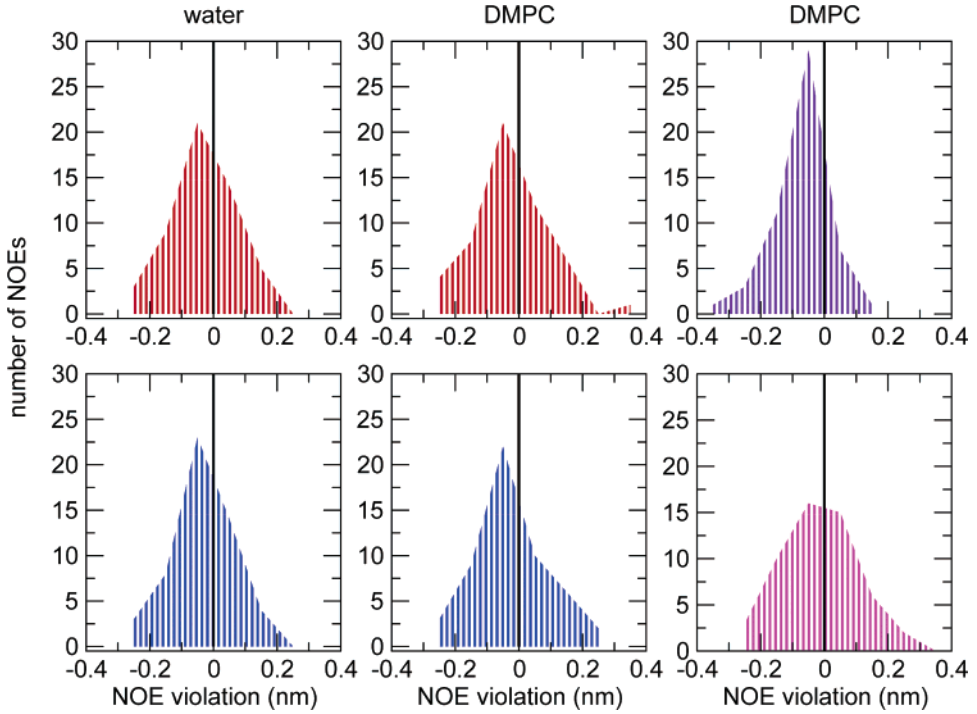

Figure 7. Number of r^{-6}-averaged interproton distances as a function of the size of the violation of the NOE upper bound. The results from the lnkn (blue) and lnkz (red) simulations in water are in the left panels, and those from the simulation at the DMPC surface in the middle panels and those from the simulations with NOE restraints applied (indigo) and released (magenta) are on the right.

appearance of turns at Gly2 and Phe4 in the neutral form of the peptide (Figure 2). The reverse change in the dihedral angle accompanied by a disruption of the turns takes place at 35 ns. The *z*-projections of the five Cα atoms are closer to each other and tend toward the nonpolar alkane tails. The ring of Tyr1 in the neutral peptide reorients along the *Z*-axis (Figure 5).

Following the time evolution of the neutral peptide at the DMPC surface, we see that there are two main events occurring, one at 25 ns and the other at 35 ns. Between 0 and 25 ns the peptide shows conformational flexibility that is related to the transitions in the Gly3 ψ dihedral angle. After 25 ns, the bend at Gly3 that appeared intermittently until then becomes a stable

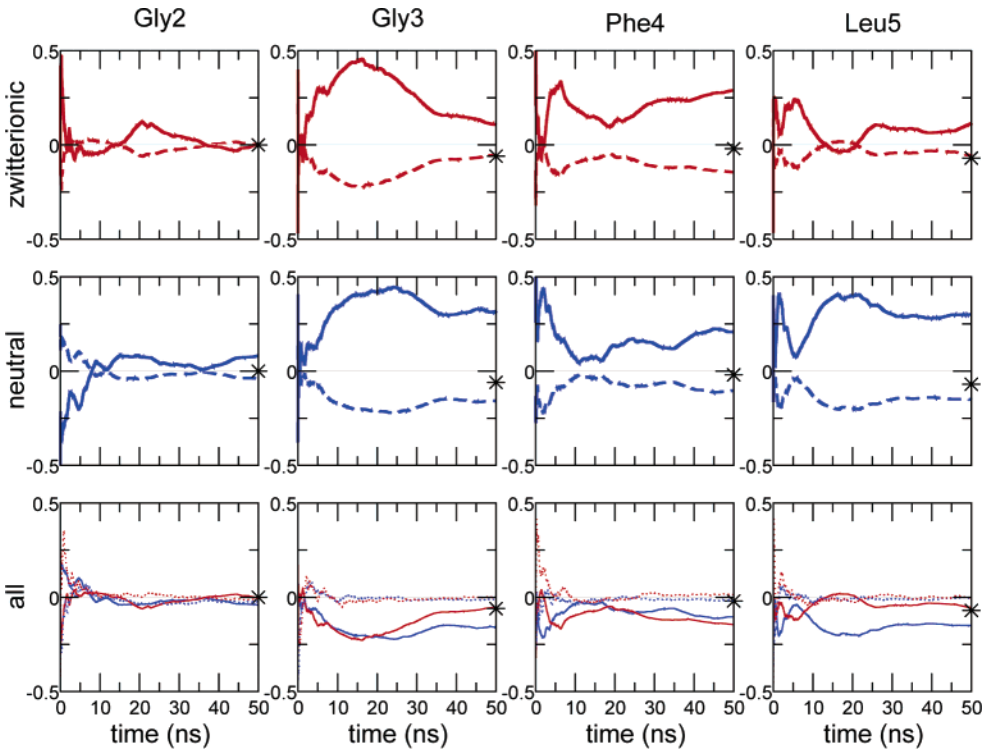

Figure 8. Running average of the P_2 Legendre function of the angle the N−H vectors of Gly2, Gly3, Phe4, and Leu5 of lenk at the DMPC surface make with the Z (normal to the bilayer) axis (solid line) and with the $X-Y$ (bilayer) plane (dashed line) as a function of time. Results from the zwitterionic form (lnkz) are shown in red in the top panels and from the neutral form (lnkn) in blue in the middle panels. The bottom panels include the results with respect to the $X-Y$ plane from both neutral (blue) and zwitterionic (red) forms in water (dotted lines) and at the membrane surface (thin solid lines). The values from experiment are shown as stars.

feature of the peptide. Between 25 and 35 ns, in addition to the bend, turns appear at Gly2 and Phe4. They are accompanied by a transition in the Gly2 ψ angle. When ψ of Gly2 changes back from 60/90° to 270/300° at 35 ns, the turns disappear. The analysis of the relative depth of the lenk molecule in the membrane provides a link in explaining the conformational behavior of the peptide. The conformational changes between 25 and 35 ns occur when the peptide reorients on the membrane surface and moves toward the polar region. The depth analysis of the remaining two simulations of the neutral peptide at the membrane surface (data not shown) support the observation that for the turns to form at residues Gly2 and Phe4, the peptide must tend toward the aqueous interface rather than toward the membrane interior. After 35 ns, the peptide is more deeply buried in the interfacial region of the membrane and the Tyr1 interacts with the hydrophobic environment, changing its orientation to align with the Z-axis. The burial of the tyrosine ring in the hydrophobic environment of the membrane has also been observed using UV resonance Raman spectroscopy, although the effect is more pronounced for menk than for lenk.[26]

3.2.3. Interproton Distances. Table 2 lists selected average interproton distances corresponding to the NOE intensities and the values calculated from the simulations using r^{-6} averaging. The selected distances correspond to "long-range" NOEs between residues separated by at least one residue. A complete table is shown in the Supporting Information. The distribution of all the interproton distance violations of the experimentally determined NOE bounds is shown in Figure 7. It should be noted that the 45A3 force field parameter set[33] that is used in the simulations has been validated for proteins against NMR data of hen egg lysozyme.[54] Despite the conformational flexibility of the peptide in water, there is no marked difference between the distribution of NOE violations in the cases of the peptide in water or at the membrane surface. These distributions suggest that many of the distances in the simulations are shorter than the NMR upper bounds. The interproton distances between the neutral and zwitterionic forms of the peptide are also similar. As might be anticipated, the simulation of the peptide with NOE distance restraints applied has the least violations (Figure 7, right panel, top). On release of the restraints, the distribution broadens and the maximum that indicates the occurrence of interproton distances of 0.1 nm shorter than the NOE upper bounds diminishes.

3.2.4. Residual Dipolar Coupling and Peptide Motion. As a consequence of the fast motion (on the NMR time scale) of the lenk molecule around the bicelle normal, the relevant angle Θ for the description of the NMR RDC according to eq 1 is the one between the ^{1}H−^{15}N vectors and the Z-axis (director) of a bicelle fixed coordinate system. The P_2 Legendre function of the angle is shown as a solid line in Figure 8, in the top panels in red for the zwitterionic and in the middle panels in blue for the neutral forms of the peptide. In addition, we have calculated the P_2 Legendre function of the angle between the ^{1}H−^{15}N vectors and the X- and the Y-axis. These two values are not identical as shown in the Supporting Information. The result is not unexpected as the long-time rotational motion of the peptide in the $X-Y$ plane that would occur on the time scale of the NMR experiment cannot be sampled during 50 ns of simulation. This is generally also the case for the long-axis

(54) Soares, T. A.; Daura, X.; Ostenbrink, C.; Smith, L. J.; van Gunsteren, W. F. *J. Biomol. NMR* **2004**, *30*, 407−422.

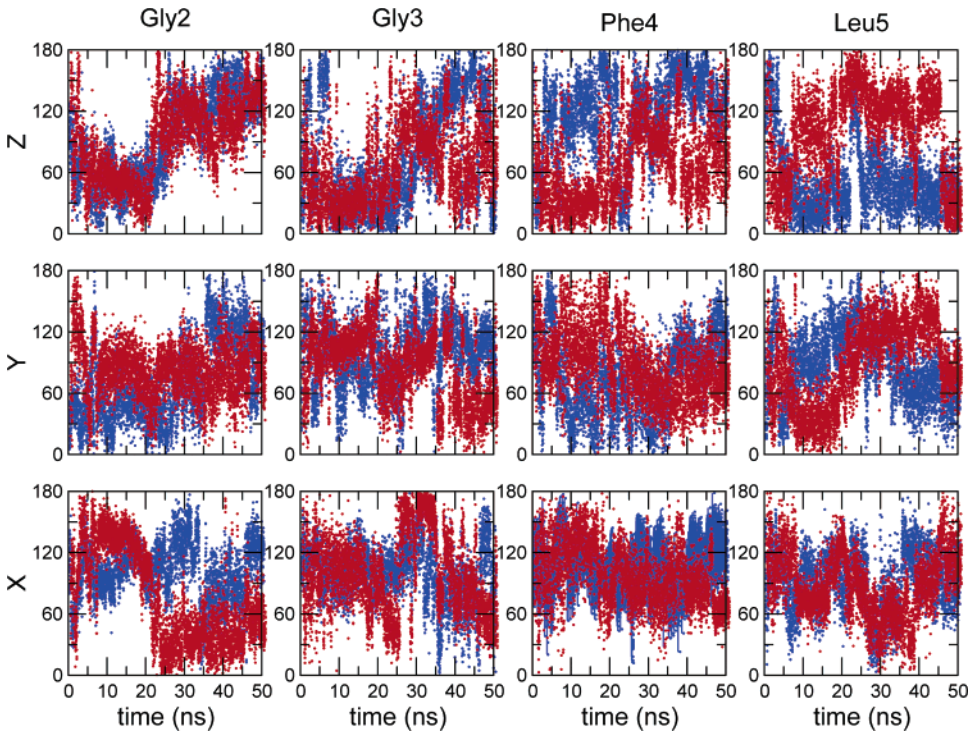

Figure 9. Angle that the N−H vectors of Gly2, Gly3, Phe4, and Leu5 of lenk at the DMPC surface make with the *X*, *Y* (in the bilayer plane), and *Z* (normal to the bilayer) axes as a function of time. Results from the neutral peptide are shown in blue and those from the zwitterionic peptide in red.

motion of the lipid molecules in simulations of the lipid bilayer on the 50 ns time scale. We therefore calculated the mean of the P_2 Legendre function of the angle an N−H vector makes with a series of axes in the $X-Y$ plane at 15° intervals. These mean values are shown as dashed lines in Figure 8. In all cases, the dashed line, which represents the function in the $X-Y$ plane, is verified to be half the mirror image of the solid line, which represents the function with respect to the *Z*-axis. Also shown, as stars, in Figure 8 are the $P_2(\cos\Theta)$ values from the NMR experiment. In both the neutral and zwitterionic cases the magnitude of the calculated P_2 Legendre function with respect to the $X-Y$ plane is significantly greater than the experimental one. There are a number of factors that could contribute to this. First, as discussed above, the simulations are short in comparison with the time scale of the NMR measurement and further processes, not covered by the additional provision for fast rotational motion around the bilayer normal (leading to a factor −0.5 in eq 1), may occur. It is known from simulations of model membranes that the long-time diffusion of lipids is also not accessed on the time scale of tens of nanoseconds.[35] Second, we make the approximation that the number of peptide molecules per bilayer, which is established to be about 0.9, is 1 during simulation. Third, the assumption that bicellar tumbling reduces the measured value by about 0.65 could also be subject to modification. Given all of the possible contributions that cannot be taken into consideration the agreement between the MD and the values from NMR is good. In the neutral case, the magnitude of the motion matches that of the NMR experiment, whereas in the zwitterionic case, the order is Phe4 > Gly3 ≅ Leu5 > Gly2 ≅ 0 (Table 3). The estimated error in all cases rounds off to 0.01, below the experimental value except in the case of Gly2 where the experimental value is 0. In the bottom panel of Figure 8, the data from the simulations of neutral (blue) and zwitterionic (red) forms of lenk in water (dotted line) and in the DMPC bilayer (solid lines) are summarized. In contrast to the simulations in the presence of the DMPC bilayer, the P_2 Legendre function of all four residues in both electronic forms of the peptide tends to 0 in the simulations in water clearly indicating that the presence of the membrane induces restricted motion in the peptide.

To determine to what extent the motion in the peptide arises from the conformational fluctuations we examined whether the orientation of the N−H vector with respect to the frame axes is related to the conformational behavior of the peptide backbone. The orientation of the respective vectors is relatively restricted in all cases. In contrast, in the water simulations (data not shown), the vectors span the range from 0° to 180°. Focusing on the neutral peptide, we know from the discussion in the subsections above that there are two major events that occur in the course of the 50 ns trajectory, one at 25 ns and the other at 35 ns. The orientations of the N−H vectors undergo transitions at one or both of these time points (Figure 9). This is particularly evident in the case of Gly2 and Gly3. For example, the transition in the ψ angle of Gly2 between 25 and 35 ns is reflected in the angle the N−H vector of Gly3 makes with respect to the *X*-axis. However, in addition to these transitions, the vectors fluctuate in a range of about 60° on a fast, picosecond time scale. These fluctuations are independent of the dihedral-angle fluctuations of the backbone. The calculated P_2 Legendre functions effectively reflect the fluctuations in the N−H vectors due to the fast librational motion, due to the dihedral-angle transitions in the backbone and due to rotational motion of the peptide about axes orthogonal to the normal to the DMPC bilayer.

4. Conclusions

The conformational and dynamic behavior of the opiate pentapeptide leucine-enkephalin is known to be profoundly affected by the presence of amphipathic membranes. Through

a combination of NMR spectroscopy and MD simulation we establish that the lenk molecule attains stable compact conformations in the presence of the DMPC bilayer. This is in contrast to lenk in the aqueous medium where the simulations indicate conformational stability over extremely short periods on the order of picoseconds. A bend at Gly3, where the ψ dihedral angle adopts staggered conformations, is the dominant conformational feature. The NMR data is consistent with two groups of structures differing at the ψ angle of Gly3. The depth penetration of the peptide in the membrane affects its conformational and orientational behavior. When the peptide moves toward the polar aqueous interface the neutral peptide forms turns at residues Gly2 and Phe4. Simultaneously, the ring of Tyr1 anchors in the hydrophobic environment of the membrane. The r^{-6}-averaged interproton distances that are compared to the NOE distance bounds are similar in the neutral and zwitterionic peptides in both aqueous medium and in the unrestrained simulations at the DMPC bilayer surface. The smallest violations, as anticipated, are in the simulation at the DMPC bilayer surface when the NOE distance restraints are applied, and the broadest distribution of violations occurs in the simulation that branches off when the NOE distance restraints are released.

In the membrane environment, the N−H vectors undergo restricted motion, fluctuating about the mean position and undergoing jumps in their orientation. The resulting P_2 Legendre functions of the angle between the N−H vector and the bilayer plane (magnetic field) lead to nonzero values in three out of the four residues both in the NMR experiment and the MD simulation. The values calculated from the MD simulation are consistently larger than the ones derived from experiment but are in the same order of magnitude. The considerable reduction of the observed RDCs compared to the full coupling of up to 22.9 kHz for a static ^{15}N−^{1}H pair is, therefore, largely explained by the dynamical averaging predicted by MD. This averaging is predominantly related to fluctuations arising from the internal flexibility of the peptide. The remaining discrepancy can probably be attributed to a combination of the approximations used in the NMR experiments concerning, for example, the bicellar tumbling motion and the fraction of lipid-associated lenk, and to the short time scale of the simulations in comparison with the NMR time scale. In the latter regard it is known that the rotational diffusion as well as translational diffusion in the plane of the bilayer and along the bilayer normal is not fully sampled. An interesting and perhaps fortuitous observation is that the relative size of the P_2 Legendre function is similar to experiment in the simulations of the neutral peptide rather than in the zwitterionic case. Although the peptide is known to be zwitterionic in aqueous medium at neutral pH, the membrane surface is highly polar and may have an influence on the electronic form of the peptide.

Acknowledgment. We thank the authors of the GROMOS^{++} analysis suite and Xavier Daura for programs that were used in the analysis and Konstantin Pervushin for the use of the high-resolution spectrometer. Financial support of the National Center of Competence in Research (NCCR) in Structural Biology of the Swiss National Science Foundation is gratefully acknowledged.

Supporting Information Available: Additional experimental details; table of the ^{1}H isotropic chemical shift assignment of lenk in isotropic bicelles at 308 K; Simulated Annealing protocol to determine NMR model structures and statistical information for the lenk structure calculation based on the NMR data; ^{1}H−^{1}H distance bounds obtained from NOE cross-peaks of lenk in isotropic bicelles at 308 K and the calculated interproton distances from the six simulations; Determination of the residual chemical-shielding anisotropy of the aromatic carbons from lenk in oriented bicelles; Ramachandran plots for all dipeptide links in each of the six MD simulations; figure showing the value of the dihedral angles, χ_1 and χ_2, linking the Tyr1 and Phe4 rings to the peptide backbone from both neutral and zwitterionic simulations as a function of time; and figure showing the running average of the P_2 Legendre function of the angle N−H vectors of residues 2−5 make with respect to the *X* and *Y* axes. This material is available free of charge via the Internet at http://pubs.acs.org.

JA054785Q